

# Seasonal variation in ~~vegetation~~grass water content estimated from proximal sensing and MODIS time series in a Mediterranean Fluxnet site

Gorka Mendiguren<sup>1,2,3,4</sup> M. Pilar Martín<sup>2,4</sup>, Héctor Nieto<sup>5</sup>, Javier Pacheco-Labrador<sup>2,4</sup>, Sara Jurdao<sup>4,6</sup>

[1] {Geological Survey of Denmark and Greenland (GEUS), Øster Voldgade 10, DK-1350 Copenhagen K, Denmark}

[2] {Instituto de Economía, Geografía y Demografía, Centro de Ciencias Humanas y Sociales, Consejo Superior de Investigaciones Científicas (CSIC), Albasanz 26-28, 28037, Madrid, Spain}

[3] {Department of Geosciences and Natural Resource Management, University of Copenhagen, Øster Voldgade 10, 1350, Copenhagen K, Denmark}

[4] {Associated Research Unit GEOLAB<sup>2 & 6</sup>}

[5] {Instituto de Agricultura Sostenible, Consejo Superior de Investigaciones Científicas (CSIC), 14080 Córdoba, Spain}

[6] {Department of Geography and Geology, University of Alcalá. Calle Colegios 2, 28801, Alcalá de Henares, Spain}

Correspondence to: Gorka Mendiguren (gmg@geus.dk)

## Abstract

This study evaluates three different metrics of ~~vegetation~~water content ~~estimated in~~ of an herbaceous cover in a Mediterranean wooded grassland (*dehesa*) ecosystem. ~~from proximal sensing and MODIS satellite imagery:~~ Fuel Moisture Content (FMC), Equivalent Water Thickness (EWT) and Canopy Water Content (CWC) ~~were estimated from proximal sensing and MODIS satellite imagery.~~ Dry matter (Dm) and Leaf area Index (LAI) ~~connect the three metrics and~~ were also analyzed. ~~in order to connect FMC with EWT and EWT with CWC,~~

1 ~~respectively. This research took place in a Fluxnet site located in a Mediterranean wooded~~  
2 ~~grassland (dehesa) ecosystem in Las Majadas del Tietar (Spain).~~ Metrics were derived from  
3 field sampling of grass cover within a 500 m MODIS pixel. Hand held hyperspectral  
4 measurements and MODIS images were simultaneously acquired and predictive empirical  
5 models were parametrized. Two methods of estimating FMC and CWC using different field  
6 protocols were tested in order to evaluate the consistency of the metrics and the relationships  
7 with the predictive empirical models. In addition, Radiative Transfer Models were used to  
8 produce estimates of CWC and FMC, which were compared with the empirical ones.

9 ~~The results indicated that FMC and EWT showed lower spatial variation than CWC.~~ Results  
10 revealed that, for all metrics spatial ~~variation~~variability was significantly lower than temporal.  
11 ~~within the MODIS pixel~~ Thus we concluded that experimental design should prioritize  
12 sampling frequency rather than sample size. ~~was not as critical as its temporal trend, so to~~  
13 ~~capture better the variability, fewer plots should be sampled but more times. Due to the high~~  
14 ~~seasonal~~Dm variability was high which demonstrate that a constant annual Dm value ~~would~~  
15 ~~not work to~~ should not be used to predict EWT from FMC as other previous studies did.  
16 Relative root mean square error (RRMSE) evaluated the performance of nine spectral indices  
17 to compute each variable. Visible Atmospherically Resistant Index (VARI) provided the  
18 ~~worst~~ lowest explicative power ~~results~~ in all cases. For proximal sensing, Global Environment  
19 Monitoring Index (GEMI) ~~worked best~~showed higher statistical relationships ~~for~~ both for  
20 FMC (RRMSE = 34.5%) and EWT (RRMSE = 27.43%) while Normalized Difference  
21 Infrared Index (NDII) and Global Vegetation Monitoring Index (GVMI) ~~performed best~~ for  
22 CWC (RRMSE =30.27% and 31.58% respectively). When MODIS data was used, results  
23 ~~were a bit better with~~showed and increase in  $R^2$  and Enhanced Vegetation Index (EVI) as the  
24 best predictor for FMC (RRMSE=33.81%) and CWC (RRMSE=27.56%) and GEMI for EWT  
25 (RRMSE=24.6%). ~~To explain these differences, proximal sensing measures only grasslands at~~  
26 ~~nadir view angle, but MODIS includes also trees, their shades, and other artifacts at up to 20°~~  
27 ~~view angle~~Differences in the viewing geometry of the platforms can explain these differences  
28 as the portion of vegetation observed by MODIS is larger than when using proximal sensing  
29 including the spectral response from scattered trees and its shadows. CWC was better  
30 predicted than the other two water content ~~variables~~metrics, probably because CWC depends  
31 on LAI, that shows a notable seasonal variation in this ecosystem. Strong statistical  
32 relationship was found between empirical models using indices sensible to chlorophyll  
33 activity (NDVI or EVI), which are not directly related to water content due to the close

relationship between LAI, water content and chlorophyll activity in grassland cover, which is not true for other types of vegetation such as forest or shrubs. ~~which is highly correlated to the spectral indices.~~ Finally, These empirical methods tested outperformed FMC and CWC products based on radiative transfer model inversion.

## 1 Introduction

Water in leaves is a limiting factor for different physiological processes of vegetation and its deficit causes malfunctioning of different cellular processes. Water is involved in the thermal regulation of plant through transpiration and also becomes crucial in the uptake of CO<sub>2</sub> for photosynthesis (Chaves et al., 2003). It is also fundamental to maintain turgor pressure, which controls different functional processes of plants like cell enlargement or gas exchange (Taiz and Zeiger, 2010).

Different metrics quantify vegetation water content. Fuel Moisture Content (FMC) (Desbois et al., 1997), defined as the mass of water per unit mass of vegetation,

$$FMC (\%) = \frac{W_{Fresh} - W_{Dry}}{W_{Dry}} * 100 \quad (1)$$

where  $W_{Fresh}$  is the fresh weight of the sample measured in the field and  $W_{Dry}$  is the oven dried weight, has been extensively used to estimate ~~the fire risk occurrence~~ and fire propagation (García et al., 2008; Yebra et al., 2008b). Equivalent Water Thickness (EWT) or Leaf Water Content (LWC), defined as the mass of water per leaf area, measures the thickness of the water layer with the same leaf area (Danson et al., 1992).

$$EWT (g/cm^2) = \frac{W_{Fresh} - W_{Dry}}{Area_{Leaf}} \quad (2)$$

where  $Area_{Leaf}$  is the leaf area.

Several studies showed that EWT can be retrieved from spectral information at leaf level as it is directly related to the water absorption depth of leaves (Ceccato et al., 2001; Datt, 1999). FMC and EWT are related each other since:

$$EWT (g/cm^2) = \left( \frac{FMC \cdot Dm}{100} \right) \quad (3)$$

where  $Dm$  is defined as the ratio of leaf dry weight and leaf area:

$$Dm \left( \text{g/cm}^2 \right) = \frac{W_{\text{Dry}}}{\text{Area}_{\text{Leaf}}} \quad (4)$$

~~EWT can be expressed as FMC multiplied by the dry matter (Dm) and divided by 100.~~

Finally, another metric is the Canopy Water Content (CWC), the mass of water in the canopy per ground area (Cheng et al., 2008; Trombetti et al., 2008). CWC represent the product of EWT and Leaf Area Index (LAI), offering information on vegetation water content at canopy level and can be expressed as:

$$CWC \left( \text{g/cm}^2 \right) = EWT \cdot LAI \quad (45)$$

or

$$CWC \left( \text{g/cm}^2 \right) = \frac{W_{\text{Fresh}} - W_{\text{Dry}}}{\text{Area}} \quad (6)$$

where Area denotes for the area of the spatial unit used to collect the sample.

~~Field sampling of FMC, EWT or CWC relies are usually estimated from vegetation samples using on-gravitational methods. but this method is quite limited for estimates at regional to global spatial scales, since it requires interpolation to bridge the gaps in both time and space.~~

Different field and laboratory protocols are used, despite of the need for standardization (Yebra et al., 2013). In several studies FMC is sampled using a bag were 100-200g of the fresh sample are introduced and considered as representative (Verbesselt et al., 2007; Chuvieco et al., 2003). In other studies vegetation is sampled within a quadrant whose area is used as reference (Sims and Gamon, 2003). However, uncertainties introduced by the different protocols and therefore their comparability are unknown. The three metrics can be used to measure water content, but relationships existing among them remains also unknown. No comparative studies for grasslands have been reported.

Moreover, field sampling is limited and cannot provide estimates at regional or global scales, since it requires interpolation to bridge the gaps in both time and space. Remote sensing is a powerful alternative data source to provide information on vegetation water content as it fills such temporal and spatial gaps. Monitoring vegetation water content with remote sensing benefits agriculture, to control crop production and prevent stress in plants (Peñuelas et al., 1992; Sepulcre-Cantó et al., 2006) and forestry, to assess fire danger associated with vegetation water conditions (Chuvieco et al., 2003; Chuvieco et al., 2004; García et al., 2008; Yebra et al., 2008b).

To estimate plant water content with remote sensing, vegetation spectral reflectance has been primarily related to specific water absorption bands in the Short Wave Infrared region (SWIR, 1300-2500 nm) (Ceccato et al., 2001; Zarco-Tejada et al., 2003). Other studies related vegetation water content to spectral indices that do not include SWIR ~~data bands. These indices monitor the vegetation water content by indirectly relating it to another biophysical parameter that is used as a proxy of water stress. This is the case of the Normalized Difference Vegetation Index (NDVI) (Tucker, 1979).~~ In the case of grass the relationship with bands in the Visible (VIS) and Near Infrared (NIR) spectral region, ~~that~~ has shown a close relationship between vegetation biomass, chlorophyll and water content ~~in grasslands~~ (Chuvieco et al., 2003; Chuvieco et al., 2004; García et al., 2008; Yebra et al., 2008b) ~~as water stress produces changes in the chlorophyll activity and biomass of the plant.~~ Least squares regression models have served to empirically relate observed measurements of ~~vegetation~~ water content to spectral indices. These models ~~have their weakest point of being~~ are site dependent, requiring long datasets for calibration (Chuvieco et al., 2009) and showing different results when the models are extrapolated to other sites using different data sets, making difficult their applicability (Riaño et al., 2005; Yebra et al., 2008a).

Radiative Transfer Models (RTM) simulate vegetation spectra and are a sound alternative to empirical modeling. They can be applied to different locations to estimate different vegetation parameters, as long as the RTM is a true representation of the vegetation canopy. For example, Trombetti et al (2008) predicted CWC for the continental US using RTM PROSAILH (Jacquemoud et al., 1995) simulations. Their model was calibrated with CWC from ~~Airborne Visible / Infrared Imaging Spectrometer (AVIRIS)~~ hyperspectral water absorption bands. Yebra et al. (2008b) ~~used also PROSAILH to quantify FMC, and more recently, Another example is~~ Jurdao et al (2013) ~~who~~ inverted the RTM GEOSAIL (Huemmrich, 2001) ~~combined with PROSAILH~~ to estimate FMC. The estimations were ~~that was~~ validated with extensive field sampling data in Spain. RTM estimates are based on a physical principle, and one of the advantages is that are not constrained to local conditions as is the case of empirically derived relationships. Therefore, in theory they can be extensively applied at different locations with good results (Yebra et al., 2008a; Yebra et al., 2008b). This study compares the ~~model~~ performance of the different empirically derived models and RTM based estimates models. The former were created ~~using~~ establishing empirical relationships between three different metrics of vegetation water content ~~measured simultaneously in the field~~ (FMC, EWT, CWC) and nine spectral indices calculated at two scales, from ~~both~~

proximal sensing and MODIS spectral data. In addition Dm and LAI were also analyzed in order to connect ~~FMC with EWT and EWT with CWC, respectively~~ metrics which estimates water content at leaf and canopy level. Firstly, an analysis of the temporal and spatial variability of the different ~~measurements~~—vegetation samples collected in the field was conducted to evaluate which biophysical parameter offers more information. Secondly, ~~the model performance was~~ the performance statistics of the fitting equations were evaluated to select the most accurate empirical models. Finally, these ~~this strategy gave us the empirical~~ models were compared to ~~two~~ three RTM based models estimates, proposed in the literature to derive ~~one two to derive~~ FMC (Jurdao et al., 2013; Yebra et al., 2008b) and the other for CWC (Trombetti et al., 2008).

## 2 Methods

### 2.1 Site description

The study site is located at Las Majadas del Tiétar (Spain) FLUXNET site (<http://fluxnet.ornl.gov/site/440>, last accessed 2014/06/05) (Fig. 1). The area is a *dehesa*, a typical Mediterranean wooded grassland, ~~which is an~~ ecosystem that occupies about 4% (2.5 Mha) of the Iberian Peninsula (Castro, 1997). Common tree species are different varieties of oaks, here mostly *Quercus ilex* subsp. *ballota* (L.), whose acorns and leaves are mainly used as forage for pigs and cows, respectively. The scattered oak trees have a 9 m mean height and 6 m mean crown diameter. Due to its deep and wide root system, this species is resistant to long drought periods (Camarero et al., 2012). Short grassland covers 86% of the area that is managed for cow shepherding. It is mainly composed by *Rumex acetosella*, L., *Plantago carinata* Schrad, *Trifolium subterraneum* L., *Cynodon dactylon* (L.) Pers., *Taraxacum dens-leonis* Desf. and *Vulpia myuros* (L.) C. C. Gmel. During the summer, grass dries out rapidly and turns into dead matter. Summers are hot and dry, with 30 °C daily average temperature and only 67 mm total precipitation, which are not representative of mean annual 16.7 °C and 572 mm. The average altitude is 256 m above mean sea level. Soils are *lixisols* with an average thickness of 80 cm. Due to the presence of a clay layer in some of the areas, small water pools may appear in winter after rainy periods. The occurrence of this type of ecosystem in Mediterranean areas worldwide, the need to track the responses to water stress

conditions, together with the presence of a FLUXNET eddy covariance flux tower (<http://fluxnet.ornl.gov/site/440>) justifies the selection of this site.

## 2.2 Field ~~sampling~~ data

### 2.2.1 Vegetation sampling

Grass water status was ~~estimated through~~ destructively ~~sampling~~ every two weeks from April 2009 to April 2011. ~~Sampling was performed~~ assuring no rain occurred in the two previous days to avoid sampling superficial water on the leaves. During the summer, ~~when~~ grass become completely dry, ~~and~~ samples were not collected in 2009. However, to ensure the time series continuity of at least one phenological cycle, sampling was restated throughout the summer of 2010. This ~~sampling~~ strategy led to a total of 21 valid sampling days for the whole study period.

Six 25 x 25 m plots were randomly located within the 500 m MODIS pixel that contained the eddy covariance flux tower ~~that was established as the center of the study site~~ (Fig. 1). Three grass samples were collected from ~~three~~ 25 x 25 cm<sup>2</sup> quadrants randomly positioned within each plot. All rooted grasses were collected inside the quadrant using clippers ( $IQ_{Sample}$  hereafter). Additionally, a ~~different sampling strategy was tested and~~ a smaller sample was collected outside of the quadrant but nearby ~~to estimate EWT~~  $EWT_{Sample}$  ~~hereafter in a cost-effective way~~, containing a representative proportion of surrounding species ( $OQ_{Sample}$  hereafter) (Fig. 2). All samples were placed in sealed plastic bags, weighed on a scale with 0.01 g precision and then transported in a cooler to the laboratory. ~~Every~~  $OQ_{Sample}$  ~~Each~~  $EWT_{Sample}$  and a sub-sample from each  $IQ_{Sample}$  were scanned at 150 pixels per inch (ppi) in an Epson Perfection V30 color scanner (Epson American Inc., Long Beach, CA, USA). Leaf area was calculated automatically from the scanned images using the unsupervised classification algorithm ISOCLUS with 16 iterations in PCI Geomatica (PCI Geomatics, Richmond Hill, Ontario, Canada). All samples were then placed in an oven for 48 hours at a constant temperature of 60°C to obtain their dry weigh. Five biophysical variables were obtained from the collected vegetation samples: FMC, EWT, Dm, CWC and LAI.

FMC was determined from the fresh and dry weights of both the  $IQ_{Sample}$  ( $FMC_{IQ}$ ) and the  $OQ_{Sample}$  ( $FMC_{OQ}$ ) according to Eq. 1. The  $OQ_{Sample}$  permitted to calculate both, EWT and Dm using Eq. 23 and Eq. 4 respectively, since fresh/dry weight and leaf area were measured. The  $IQ_{Sample}$  was not used in this case as it was unfeasible to obtain the area of the total sample



collected inside the quadrant and neither the fresh weight of a sub-sample.  ~~FMC was determined from the fresh and dry weights of both the whole quadrant sample (FMC<sub>Q</sub>) and the EWT<sub>Sample</sub> (FMC<sub>E</sub>) according to Eq. 1. The EWT<sub>Sample</sub> permitted to calculate both, EWT and Dm, since fresh/dry weight and leaf area were all measured) of the EWT<sub>Sample</sub>.~~

CWC was calculated from two different approaches. In the first one, information corresponding to the ~~quadrant and EWT<sub>Sample</sub>~~ IQ<sub>sample</sub> and OQ<sub>sample</sub> were combined using the following expression (Eq. 5) ~~where LAI is the leaf area index of the grass within the quadrant and EWT is obtained from Eq 2.~~

The grass height was very short due to cow shepherding during some periods, so the only feasible technique to estimate LAI, ~~rather than optically estimated, was measured with~~ was using gravitational methods (He et al., 2007). The biomass to leaf area ratio of a sub-sample inside the IQ<sub>Sample</sub> to the total quadrant's biomass provided LAI using the following expression (Eq 5):

$$LAI(\text{cm}^2/\text{cm}^2) = \frac{\frac{W_{\text{Dry}}}{W_{\text{Dry}}^{\text{Sub}}} \text{Area}_{\text{Leaf}}^{\text{Sub}}}{\text{Area}} \quad (7)$$

where W<sub>Dry</sub> is the total dry weight of the whole sample inside the ~~quadrant~~ IQ<sub>Sample</sub>, W<sub>Dry</sub><sup>Sub</sup> is the dry weight of a sub-sample of W<sub>Dry</sub>, Area<sub>Leaf</sub><sup>Sub</sup> is the sub-sample leaf area and Area is the total area of the quadrant. The second approach measured CWC from the fresh and dry weight difference of the IQ<sub>Sample</sub> as in (Eq. 6).

~~The second approach measured CWC from the fresh and dry weight difference inside the quadrant (CWC<sub>Q</sub> in Eq. 6):~~

## 2.2.2 Proximal sensing

Simultaneously to vegetation sampling, proximal sensing data were acquired using an ASD FieldSpec® 3 spectroradiometer (<http://www.asdi.com/>) along NE-SW and NW-SE transects in each 25x25 m plot. This instrument measures Hemispherical-Conical Reflectance Factor (HCRF) reflectance from 350 to 2500 nm. Before measuring along each transect, dark current was recorded, instrument settings were optimized and reference spectra were acquired using a Spectralon® 99% reflective reference panel (Labsphere Inc., North Sutton, NH, USA). All



measurements were taken under clear sky within about  $\pm 2$  hours from local solar noon, to guarantee homogeneous illumination and maximum solar irradiance. Sky conditions were recorded in the field logs, and a quality control check removed the spectra where illumination changes may have occurred after calibration. The ASD was handled using bare fiber, ~~without fiber optics to reduce the directional effects on the spectroradiometer's fiber bundle field of view (FOV) (MacArthur et al., 2012).~~ Spectra were acquired at approximately 1.2 m height, rendering a sensor footprint diameter of about 53 cm, since nominal FOV is 25°.

An average of approximately 10 spectral measurements was calculated for each transect and ~~then this information was~~ spectrally resampled to MODIS bands using ITT ENVI 4.7. (EXELIS, Boulder CO, USA). ~~(Paltridge and Barber, 1988; Yebra et al., 2008b). Finally, two RTM-based algorithms were run to compare with these spectral indices. GEOSAIL RTM model inversion estimated FMC testing two different look up tables that constrained the simulations to either a grassland or a mixed tree grassland cover based on Jurdao et al. (2013). PROSAILH RTM model inversion predicted CWC assuming a pure grassland cover following Trombetti et al. (2008). This model applies the same look up table to all land covers but different calibration coefficients which will render the same  $R^2$  independently of the land cover considered.~~

### 2.2.3 MODIS data images

MODIS Terra daily surface reflectance (MOD09GA) data from April 1st, 2009 to April 15th, 2011 were downloaded from NASA Land Processes Distributed Active Archive Center (LP DAAC) at the USGS/Earth Resources Observation and Science (EROS) Center, Sioux Falls, South Dakota, USA. This product includes the reflectance of bands 1 to 7, from 469 to 2130 nm at 500 m spatial resolution, as well as sensor and solar observation angles and quality flags at 1 km. A script programmed in Matlab (Mathworks, Batick, Massachusetts, USA) extracted the MODIS pixel value of our study site from all the images to build the time series. The impact of angular effects on reflectance was reduced by removing images with sensor zenith angles wider than 20°, which also assures the accuracy of the geometrical location of the pixel (Wolfe et al., 2002). In addition, the quality flag layer eliminated images under clouds, cloud shadows and/or with high atmospheric aerosol content. The algorithm selected the closest valid MODIS image to the field sampling day within  $\pm 5$  days window, or the MODIS image acquired before the sampling day in case they were equal. Minimal time lag between sensor and field data reduces the chances of discrepancy, as grassland grazing could

1 affect LAI in a short period of time. This led to a total of 14 days of MODIS data with  
2 coincident proximal sensing measurements and field data.

3 ~~Similarly to proximal sensing, MODIS estimated the biophysical variables from the spectral~~  
4 ~~indices in Table 1 and from the RTM model inversions.~~

## 5 **2.3 Vegetation indices**

6 ~~These~~ For the study 9 spectral indices were calculated from proximal and MODIS reflectance  
7 data according to the equations in Table 1. The indices selected to estimate the biophysical  
8 variables included bands in the water absorption SWIR region (Faurtyot and Baret, 1997) and  
9 bands sensitive to vegetation greenness and structure in the NIR region (Paltridge and Barber,  
10 1988; Yebra et al., 2008b).

## 11 **2.4 RTM based water metrics estimates**

12 In order to compare performance with the empirical derived models, three RTM based models  
13 were used to estimate CWC (Trombetti et al., 2008) and FMC (Yebra et al. (2008b); Jurdao et  
14 al. (2013)). As for the empirical models, the spectral information used to run the RTMs was  
15 the one obtained using proximal sensing and MODIS data.

### 16 **2.4.1 CWC**

17 CWC was estimated in the study site following Trombetti et al. (2008). This method uses  
18 PROSAILH RTM (Jacquemoud and Baret, 1990; Jacquemoud et al., 1995) and Artificial  
19 Neural Networks (ANN) to estimate CWC. Trombetti et al. (2008) trained their model by  
20 using MODIS synthetic spectra based on a set of empirical relationships. Different MODIS  
21 spectra combinations and vegetation indices were later used as input variables to train a neural  
22 network and obtaining as outputs CWC, leaf water content, and LAI. The outputs were  
23 validated against AVIRIS CWC and MODIS MOD15A2 LAI product. ~~At the end, a~~ Multiple  
24 linear regression approach is later used to establish the equations for each landcover type. In  
25 our case we used the original calibration from Trombetti et al. (2008) for grassland.

26 Further details on this method can be found in Trombetti et al. (2008).

## 2.4.2 FMC

The FMC estimates are based on Look Up Table (LUT) inversion technique. This technique compares each observed spectra against previously generated spectra stored in a LUT. In this study two LUTs were tested. One specifically designated for grassland based on the study of Yebra et al. (2008b) and that was generated using PROSAILH (Jacquemoud and Baret, 1990). The second LUT was generated using a link between PROSAILH (Jacquemoud and Baret, 1990) at leaf level and GEOSAIL RTM (Huemmrich, 2001) at canopy level and originally proposed to estimate FMC in a mixed-oak-tree-grassland cover (Jurdao et al., 2013). This model includes some additional parameters that allow to account for shadows, especially important in areas with disperse tree coverage as is the case in our study site.

Further details on these methods can be found in Yebra et al. (2008b) and Jurdao et al. (2013).

## 2.5 Data-analysis Empirical models fitting

Intra-group, inter-group and overall  $R^2$  values between  $FMC_{IQ}$ ,  $FMC_{OQ}$ , EWT,  $CWC_{IQ}$ ,  $CWC_{OQ}$  or LAI, and each of the proximal sensing spectral indices were calculated to investigate their variability within the 500 m MODIS pixel. More specifically, the intra-group  $R^2$  offers information about the spatial variability, due to the collection of samples ~~at~~ from different plots within the MODIS pixel. A linear regression model was created for each sampling day where the biophysical variable and the spectral index were the dependent and the independent variable, respectively. The average  $R^2$  of all the regression models for each day provided the intra-group  $R^2$ . Instead, the inter-group  $R^2$  explains the temporal variability due to the collection of the samples on different days. In this case, the biophysical variable and the spectral index for all plots were averaged for each sampling day. The linear regression model of these averaged values determined the inter-group  $R^2$ . To explain temporal and spatial variability together, the overall  $R^2$  fitted in a single regression model including all plots and sampling days for each spectral index and biophysical variable.

Later, using the mean values of each biophysical variable and the proximal sensing spectral indices, a univariate linear regression model was applied. The same procedure was repeated for MODIS data. Bootstrapping techniques evaluated the empirical model robustness, which is a valid alternative to traditional leave-one-out methods to validate regression models predictability according to Richter et al. (2012) and following Steyerberg et al. (2001) that

recommends two hundred simulations. Later the median value of each statistics was used as indicative of its performance. Root Mean Square Error (RMSE), Relative Root Mean Square Error (RRMSE), ~~Nash-Sutcliffe Efficiency index (NSE)~~, determination coefficient ( $R^2$ ) and Taylor's diagrams evaluated the models' performance. ~~As recommended in Steyerberg et al. (2001), two hundred bootstrap model simulations were run for each model and the median value of each statistics represented its performance.~~ The RMSE measured the error in the estimation of the biophysical variable by each model:

$$\text{RMSE} = \sqrt{\frac{1}{n} \sum_{i=1}^n (V_{\text{est}}^i - V_{\text{obs}}^i)^2} \quad (8)$$

Where  $V_{\text{est}}^i$  is the estimated variable and  $V_{\text{obs}}^i$  is its observed field measurement. RMSE cannot compare the error of different variables with different units. To address this limitation in order to compare the model performances between different variables, RRMSE divides RMSE by the average of the observed values  $\bar{V}_{\text{obs}}$  (Richter et al., 2012):

$$\text{RRMSE} = 100 \frac{\text{RMSE}}{\bar{V}_{\text{obs}}} \quad (9)$$

~~The NSE indicates the model predictive power which ranges from  $-\infty$  to the best predictive power value of 1 (Richter et al., 2012). It establishes if the model performs at least as accurate as the average of observed values through the following expression:~~

~~$$\text{NSE} = 1 - \frac{\sum_{i=1}^n (V_{\text{est}}^i - V_{\text{obs}}^i)^2}{\sum_{i=1}^n (V_{\text{obs}}^i - \bar{V}_{\text{obs}})^2} \quad (9)$$~~

The  $R^2$  measures the proportion of variance explained by the model and is calculated as:

$$R^2 = 1 - \frac{\sigma_r^2}{\sigma^2} \quad (10)$$

where  $\sigma_r^2$  represents the residual variance and  $\sigma^2$  is the variance of the dependent variable.

## 2.6 Comparing performance between empirical and RTM based estimates

Taylor diagrams allowed the comparison between the ~~spectral indices~~ FMC and CWC predicted by empirical models fit and the RTM inversion estimates ~~based algorithms of~~

Jurdao et al. (2013) ~~and Trombetti et al. (2008)~~ for FMC and CWC, respectively. In these plots the observed variable and its standard deviation (*SD*) are plotted in the x-axes. RMSE is represented as semicircles centered at the observed data. The correlation coefficient (*r*) is displayed in the azimuthal position. Best models are closer in the plot to the observed measurement; therefore they will have a high *r*, a low RMSE and a SD similar to the observed values.

### 3 Results

#### 3.1 Empirical models fitting

All variables showed similar temporal evolution, a strong variability controlled by the meteorological conditions with a peak in spring and second minor peak in the ~~fall~~ winter except Dm (Fig. 3). Dm fluctuated throughout the year and exhibited its highest values in the summer. The 47% Coefficient of Variation (CV) for Dm was less than for CWC<sub>IQ</sub> (CV= 95%), CWC<sub>OQ</sub> (CV=0.95%), FMC<sub>IQ</sub> (CV= 60%) and FMC<sub>OQ</sub> (CV= 56%), but higher than for EWT (CV= 38%). A higher precipitation in the spring of 2010 ~~versus the previous year~~ compared to previous year translated into higher FMC, CWC and LAI values. FMC<sub>OQ</sub> and CWC<sub>OQ</sub>, calculated from the ~~EWT<sub>Sample</sub>~~ ~~OQ<sub>Sample</sub>~~, presented similar trends but in some cases higher values than FMC<sub>IQ</sub> and CWC<sub>IQ</sub>, calculated from the ~~quadrant sample~~ ~~IQ<sub>Sample</sub>~~.

A low intra-group  $R^2$  for all the variables indicates a low spatial variability between plots (Fig. 4). Contrary, the high inter-group  $R^2$  also for all variables points to the high temporal variability between sampling dates. The main differences between variables occurred for overall  $R^2$ . Similar overall and inter-group  $R^2$  values for CWC<sub>OQ</sub> and FMC<sub>OQ</sub> indicated that the combination of the temporal and spatial factors matched in importance each factor on its own. Instead, overall  $R^2$  for CWC<sub>IQ</sub> and FMC<sub>IQ</sub> laid in between the inter-group and the intra-group  $R^2$  underling the temporal factor as the main source of variation. GEMI offers the best  $R^2$  for all variables while VARI had the weakest  $R^2$ .

The ~~most accurate univariate~~ ~~explicative empirical bootstrap~~ model with the highest  $R^2$  to retrieve each variable differed ~~from~~ ~~between~~ proximal sensing and MODIS (Fig. 5) ~~to MODIS (Fig. 5)~~. FMC<sub>OQ</sub> and FMC<sub>IQ</sub> showed the best correlations with GEMI from proximal sensing data but EVI ~~performed better~~ was the index that presented the highest  $R^2$  when using ~~from~~ MODIS images. EWT offered the poorest adjustments among all variables analyzed

both for proximal sensing and MODIS data. In this case GEMI was the best predictor. ~~was more accurately estimated with GEMI from either sensor but presented the lowest  $R^2$  and NSE of all the biophysical variables.~~ NDII and GVMI were the most accurate predictors for LAI,  $CWC_{OQ}$  and  $CWC_{IQ}$  with proximal sensing. When using MODIS, the most accurate results for LAI were achieved with NDII and GVMI, but EVI did so for  $CWC_{OQ}$  and  $CWC_{IQ}$ . When the ~~quadrant sample~~  $IQ_{sample}$  was used instead of the ~~EWT<sub>sample</sub>~~  $OQ_{sample}$ , both FMC and CWC showed ~~more accurate~~ higher  $R^2$  results (Fig. 5) with lower RRMSE ~~and higher NSE and  $R^2$ ,~~ although the RRMSE results obtained presented small differences (Fig. 5). Smaller confidence intervals of  $R^2$  were observed when proximal sensing reflectance was used with the exception of EWT in which MODIS presented smaller intervals.

### 3.2 Comparing performance between empirical based and RTM estimates

Taylor diagrams in Figs. 7 and 8 compare FMC and CWC estimates using spectral indices and RTM ~~using the Taylor diagrams.~~ In the case of  $FMC_{IQ}$  from proximal sensing (Fig. 7 left), RTMs are distant from empirical index-based models. They presented higher RMSE and lower  $r$  than the spectral indices whereas RTM SD was more similar to the observed values. In the case of  $FMC_{IQ}$  estimated from MODIS (Fig. 7 right), RTMs ~~was~~ were closer to the empirical models in the Taylor diagram and therefore perform more similar to those. For  $CWC_{IQ}$  (Fig. 8), the differences between the empirical and RTMs are larger. Using ~~from~~ proximal sensing data (Fig. 8 left), RTM overestimated the SD of the observed  $CWC_{IQ}$ . ~~At~~ Using MODIS ~~scale~~ (Fig. 8 right), RTM showed a very high overestimation of the  $CWC_{IQ}$ .

Temporal evolution of the biophysical variables estimated using the most ~~accurate~~ ~~explicitive~~ model for proximal sensing and MODIS in Fig. 5 and 6 are shown in Fig. 9. Fitting equations for the different variables are shown in Table 2. Both sensors predicted well EWT,  $FMC_{IQ}$  and  $FMC_{OQ}$  but showed an overestimation, especially during the dry season. Contrary, the models for LAI,  $CWC_{OQ}$  and  $CWC_{IQ}$  adjusted well even during the dry season.

## 4 Discussion

Results revealed that Dm varies significantly throughout the year ( $CV=47\%$ ) with high values in the summer. These changes could be related to the temporal variation in plant community structure, species composition and diversity in this ecosystem (Casado et al.,

1986). Summer should be the best time of the year to invert RTM and predict Dm, since leaves are drier and therefore EWT does mask the Dm spectral absorption signal (Riaño et al., 2005). Casas et al. (2014) applied a constant annual Dm value from the literature to successfully predict seasonal variations in EWT and CWC. However, our study suggests that, due to the high seasonal variation in Dm, a constant annual value would not be recommended here in grassland ecosystems as the one analyzed in this work.

The high inter-group and low intra-group  $R^2$  implies that the temporal trend is much more critical than the spatial variation within the MODIS pixel (Fig. 4). ~~Therefore, the strategy to capture better the variability of vegetation water content in this ecosystem should be to sample more times but fewer plots.~~ Therefore, the strategy to better capture the variability of grass water content in this ecosystem should consist in increasing the number of samples in time and but sampling less number of plots per day. In addition,  $CWC_{IQ}$  and  $FMC_{IQ}$ , generated from larger sample sizes than  $CWC_{OQ}$  and  $FMC_{OQ}$ , presented higher inter-group  $R^2$  values, which indicate a better characterization of the temporal variability. Even though similar conclusions were obtained using the two strategies the results in this study showed that the higher  $R^2$  are found in the case of the  $IQ_{Sample}$ . Using the quadrant also presented some advantages as it allows not just the retrieval of FMC but also CWC (as in Eq. 6) without going through the time consuming leaf scanning process to retrieve leaf area needed to estimate EWT. This suggests the need to standardize sampling protocols for the estimation of vegetation biophysical parameters to ensure data quality, repeatability and to facilitate accurate cross comparison from different studies. Some initiatives already exist to facilitate this standardization, as the Global Terrestrial Carbon System (GTOS) guidelines in support of carbon cycle science (Law et al., 2008). However, currently there is no international backbone that ensures this and an agreement in the protocols is needed in order to validate remote sensing products.

CWC was better predicted than the other two water content ~~variables-metrics~~, FMC and EWT (Fig. 4). CWC depends on LAI which is ~~even higher correlated~~ showing higher correlation values to the empirical models than ~~those two variables~~ other metrics such as FMC or EWT. Some studies have shown that LAI contributions to total reflectance variability is much higher than water (Bowyer and Danson, 2004) for this reason also, CWC should provide more accurate retrievals than FMC or EWT. It is possible to have the same FMC and EWT for different LAI and hence different CWC and amount of soil background, which will change its



reflectance. Yebra et al. (2013) demonstrated through PROSAILH simulations how a very different CWC for the same EWT based on changes of LAI translates into a ~~huge~~-large range of NDII values. Our results confirm this theoretical assumption described in Yebra et al. (2013). This issue is especially critical over areas like ~~this one~~ the one analyzed in this work with an herbaceous cover exhibiting large dynamic annual growth. Very low  $R^2$  values were obtained in this study regarding the EWT. More research needs to be done in this line as EWT is a key input parameter in many RTM.

The empirical methods estimated FMC and CWC with slightly different results for proximal sensing and MODIS (Figs. 5 and 6). While GEMI and NDII were the most accurate for FMC and CWC respectively from proximal sensing in our study; EVI was the most accurate explicative estimator of both variables from MODIS. The relationship between these indices and water metric is indirect, since none of them include spectral bands in the SWIR region where water absorption is strong. However, there is a strong link between grass water content, chlorophyll activity and LAI in this ecosystem. During wet periods the grass grows very rapidly, increasing the LAI, biomass and chlorophyll content, but as soon as the dry season starts with high temperatures and low rainfall the grass becomes cured rapidly losing all chlorophyll and quickly decreasing the LAI and biomass. This explains the empirical relationships with high  $R^2$  between water metrics and indices sensible to chlorophyll activity, or those more sensible to water in the SWIR region. In addition, it is remarkable that MODIS estimations ~~were more accurate~~ presented higher  $R^2$  than proximal sensing. Bootstrap confidence intervals indicated that  $R^2$  and RRMSE presented large intervals, larger when using MODIS images. Roberts et al. (2006) also observed different correlations between indices and platforms and the discrepancies here need further investigation. The difference in the confidence interval amplitude between proximal sensing and MODIS can be explained because the MODIS pixel included not only grass but also trees, their shades, and other marginal covers like bare soil and a water pond (Fig. 1), and its view angle could be up to 20° whilst proximal sensing measures only two transects within each of the six plots and provides only nadir measurements of herbaceous cover which could be more affected by the soil signal.

Similarly to this study, Casas et al. (2014) reliably predicted water content variables in California (USA) from GEMI, NDII and EVI using simulated MODIS spectral response from airborne hyperspectral AVIRIS instrument. In their case, it was actually VARI the most

accurate for grasslands (FMC and CWC), chaparral (EWT, FMC and CWC) and a Mediterranean oak forest (EWT). Contrary, VARI showed very poor accuracies in our case to estimate FMC, EWT and CWC, but was still capable of capturing the variability in LAI (Fig. 4). This fact also contradicts other studies that predicted FMC from VARI on chaparral (Peterson et al., 2008; Roberts et al., 2006; Stow et al., 2005, 2006). VARI was developed to detect vegetation fraction in homogenous wheat crops (Gitelson et al., 2002b), but Gitelson et al. (2002a) nor the above studies have tested this spectral index to detect vegetation water content on sites like ours, with strong seasonal changes in species composition and LAI.

The empirical methods calibrated for this specific site outperformed the physical RTM estimates for CWC and FMC (Figs. 4 and 5). This confirms the results in Casas et al. (2014) where the CWC algorithm based on RTM inversion developed by Trombetti et al. (2008) also failed to improve results from empirical estimates. Regarding the RTM-based-FMC estimates, considering that the FMC inversion models were not calibrated with any data from the field campaign and that the results were similar to those obtained using empirical approach (Fig. 7) we believe that the models can be applied in other similar areas. ~~RTM-only overcome when structural information constrains the model inversion (Yebra et al., 2008b; Casas et al., 2014). Such ancillary information is key to successfully extrapolate a RTM inversion at broader scale.~~

Future work in this line can still be done, testing other inversion techniques, using multiple observations or other optimization algorithms might help to improve the performance of physical based estimates of biophysical variables of vegetation.

## 5 Conclusions

This work showed a complete analysis of three metrics, EWT, FMC and CWC, to measure ~~vegetation~~-grass water content at two different spatial scales by using proximal sensing from a field spectroradiometer and MODIS images. The temporal changes in these metrics are more critical than their spatial variation within the MODIS pixel. Results indicated that larger samples collected using quadrants as spatial reference sampling units are more representative than the small ~~EWT<sub>Sample</sub>~~- samples in order to follow the temporal trends in FMC and CWC.. Protocol standardization ~~in order to make different datasets comparable~~ should be considered

1 to make different dataset comparable both spatially and temporally. Due to the high seasonal  
2 Dm variability, a constant annual value should not be used to estimate EWT from FMC in this  
3 ecosystem. The dependence of CWC on LAI makes this vegetation water content variable  
4 easier to predict than FMC or EWT in grasslands due to the strong existing link between LAI,  
5 water content and chlorophyll activity.

6 GEMI, NDII and EVI reliably predicted vegetation water content. The best empirical  
7 estimator differed between sensors. Empirical models based on vegetation indices Results  
8 were a bit better showed higher  $R^2$  for MODIS than from proximal sensing, probably due to  
9 differences induced by observation geometry and canopy observed in view angles, sampling  
10 strategy and canopy observed. These empirical methods still exceed RTM inversions  
11 developed for other sites to predict FMC (Jurdao et al., 2013; Yebra et al., 2008b) and CWC  
12 (Trombetti et al., 2008). Conclusions from this study are much related to grassland physiology  
13 and cannot be extended to other vegetation types such as forest or shrubs.

#### 14 **Acknowledgements**

15 This study has been carried out in the context of the BIOSPEC (CGL2008-02301) and  
16 FLUXPEC (CGL2012-34383) projects funded by the Spanish Ministry of Science and  
17 Innovation and the Ministry of Economy and Competiveness respectively and the  
18 SENSORVEG (FP7-PEOPLE-2009-IRSES) action. The FPI grant program supported Gorka  
19 Mendiguren predoctoral research (BES-2009-026831) as well as short stays at the University  
20 of Copenhagen during year 2011 (EEBB-2011-44463) and 2012 (EEBB-I-12-04542) and to  
21 Rasmus Fensholt for hosting in the department. All the people involved in the field work  
22 campaigns from different institution: Spanish Council for Scientific Research, University of  
23 Alcalá de Henares, University of Zaragoza, CEAM and Instituto Nacional de Investigaciones  
24 Agrarias (INIA) are acknowledged. Collaboration with NASA Terrestrial Hydrology Program  
25 (grant # NNX09AN51G) and David Riaño for his comments and suggestions are also  
26 acknowledged. The first author would like to thank Spanish INEM for its funding support.

## 1    References

- 2    Bowyer, P., and Danson, F. M.: Sensitivity of spectral reflectance to variation in live fuel  
3    moisture content at leaf and canopy level, *Remote Sensing of Environment*, 92, 297 - 308,  
4    2004.
- 5    Camarero, J. J., Olano, J. M., Arroyo Alfaro, S. J., Fernández-Marín, B., Becerril, J. M., and  
6    García-Plazaola, J. I.: Photoprotection mechanisms in *Quercus ilex* under contrasting climatic  
7    conditions, *Flora: Morphology, Distribution, Functional Ecology of Plants*, 207, 557-564,  
8    2012.
- 9    Casado, M. A., de Miguel, J. M., Sterling, A., Peco, B., Galiano, E. F., and Pineda, F. D.:  
10    Production and spatial structure of Mediterranean pastures in different stages of ecological  
11    succession, *Vegetatio*, 64, 75-86, 10.1007/BF00044783, 1986.
- 12    Casas, A., Riaño, D., Ustin, S. L., Dennison, P., and Salas, J.: Estimation of water-related  
13    biochemical and biophysical vegetation properties using multitemporal airborne hyperspectral  
14    data and its comparison to MODIS spectral response, *Remote Sensing of Environment*, 148,  
15    28-41, <http://dx.doi.org/10.1016/j.rse.2014.03.011>, 2014.
- 16    Castro, E. B.: *Los Bosques Ibéricos: Una Interpretación Geobotánica*, Editorial Planeta S. A.  
17    Barcelona, 1997.
- 18    Ceccato, P., Flasse, S., Tarantola, S., Jacquemoud, S., and Grégoire, J.-M.: Detecting  
19    vegetation leaf water content using reflectance in the optical domain, *Remote Sensing of*  
20    *Environment*, 77, 22 - 33, 2001.
- 21    Ceccato, P., Gobron, N., Flasse, S., Pinty, B., and Tarantola, S.: Designing a spectral index to  
22    estimate vegetation water content from remote sensing data: Part 1: Theoretical approach,  
23    *Remote Sensing of Environment*, 82, 188 - 197, 2002.
- 24    Chaves, M. M., Maroco, J., #227, P., o., Pereira, J., and S., o.: Understanding plant responses  
25    to drought from genes to the whole plant, *Functional Plant Biology*, 30, 239-264,  
26    <http://dx.doi.org/10.1071/FP02076>, 2003.
- 27    Cheng, Y.-B., Ustin, S. L., Riaño, D., and Vanderbilt, V. C.: Water content estimation from  
28    hyperspectral images and MODIS indexes in Southeastern Arizona, *Remote Sensing of*  
29    *Environment*, 112, 363 - 374, 2008.
- 30    Chuvieco, E., Aguado, I., Cocero, D., and Riaño, D.: Design of an empirical index to estimate  
31    fuel moisture content from NOAA-AVHRR images in forest fire danger studies, *International*  
32    *Journal of Remote Sensing*, 24, 1621-1637, 2003.
- 33    Chuvieco, E., Cocero, D., Riaño, D., Martín, P., Martínez-Vega, J., de la Riva, J., and Pérez,  
34    F.: Combining NDVI and surface temperature for the estimation of live fuel moisture content  
35    in forest fire danger rating, *Remote Sensing of Environment*, 92, 322 - 331, 2004.
- 36    Chuvieco, E., Wagtendok, J., Riaño, D., Yebra, M., and Ustin, S.: Estimation of fuel  
37    conditions for fire danger assessment, in: *Earth observation of wildland fires in Mediterranean*  
38    *ecosystems*, Springer, Berlin Heidelberg, 83-96, 2009.
- 39    Danson, F., Steven, M. D., Malthus, T. J., and Clark, J. A.: High-spectral resolution data for  
40    determining leaf water content, *International Journal of Remote Sensing*, 13, 461-470, 1992.
- 41    Datt, B.: Remote sensing of water content in Eucalyptus leaves, *Australian Journal of Botany*,  
42    47, 909-923, 1999.

- 1 Desbois, N., Deshayes, M., and Beudin, A.: A Review of Remote Sensing Methods for the  
2 Study of Large Wildland Fires, edited by: Chuvieco, E., Protocol for fuel moisture content  
3 measurements, 61-72 pp., 1997.
- 4 Faurtyot, T., and Baret, F.: Vegetation water and dry matter contents estimated from top-of-  
5 the-atmosphere reflectance data: A simulation study, Remote Sensing of Environment, 61, 34-  
6 45, [http://dx.doi.org/10.1016/S0034-4257\(96\)00238-6](http://dx.doi.org/10.1016/S0034-4257(96)00238-6), 1997.
- 7 Gao, B.-c.: NDWI A normalized difference water index for remote sensing of vegetation  
8 liquid water from space, Remote Sensing of Environment, 58, 257 - 266, 1996.
- 9 García, M., Chuvieco, E., Nieto, H., and Aguado, I.: Combining AVHRR and meteorological  
10 data for estimating live fuel moisture content, Remote Sensing of Environment, 112, 3618 -  
11 3627, 2008.
- 12 Gitelson, A. A., Kaufman, Y. J., Stark, R., and Rundquist, D.: Novel algorithms for remote  
13 estimation of vegetation fraction, Remote Sensing of Environment, 80, 76-87, 2002a.
- 14 Gitelson, A. A., Stark, R., Grits, U., Rundquist, D., Kaufman, Y., and Derry, D.: Vegetation  
15 and soil lines in visible spectral space: A concept and technique for remote estimation of  
16 vegetation fraction, International Journal of Remote Sensing, 23, 2537-2562,  
17 10.1080/01431160110107806, 2002b.
- 18 Hardisky, M. A., Klemas, V., and Smart, R. M.: The influence of soil salinity, growth form,  
19 and leaf moisture on the spectral radiance of *Spartina alterniflora* canopies, Photogrammetric  
20 Engineering & Remote Sensing, 49, 77-83, 1983.
- 21 He, Y., Guo, X., and Wilmshurst, J. F.: Comparison of different methods for measuring leaf  
22 area index in a mixed grassland, Canadian Journal of Plant Science, 87, 803-813,  
23 10.4141/cjps07024, 2007.
- 24 Huemmrich, K. F.: The GeoSail model: a simple addition to the SAIL model to describe  
25 discontinuous canopy reflectance, Remote Sensing of Environment, 75, 423-431,  
26 [http://dx.doi.org/10.1016/S0034-4257\(00\)00184-X](http://dx.doi.org/10.1016/S0034-4257(00)00184-X), 2001.
- 27 Huete, A.: A soil-adjusted vegetation index (SAVI), Remote Sensing of Environment, 25, 295  
28 - 309, 1988.
- 29 Huete, A., Didan, K., Miura, T., Rodriguez, E. P., Gao, X., and Ferreira, L. G.: Overview of  
30 the radiometric and biophysical performance of the MODIS vegetation indices, Remote  
31 Sensing of Environment, 83, 195 - 213, 2002.
- 32 Jacquemoud, S., and Baret, F.: PROSPECT: A model of leaf optical properties spectra,  
33 Remote Sensing of Environment, 34, 75-91, [http://dx.doi.org/10.1016/0034-4257\(90\)90100-](http://dx.doi.org/10.1016/0034-4257(90)90100-Z)  
34 [Z](http://dx.doi.org/10.1016/0034-4257(90)90100-Z), 1990.
- 35 Jacquemoud, S., Baret, F., Andrieu, B., Danson, F. M., and Jaggard, K.: Extraction of  
36 vegetation biophysical parameters by inversion of the PROSPECT + SAIL models on sugar  
37 beet canopy reflectance data. Application to TM and AVIRIS sensors, Remote Sensing of  
38 Environment, 52, 163-172, [http://dx.doi.org/10.1016/0034-4257\(95\)00018-V](http://dx.doi.org/10.1016/0034-4257(95)00018-V), 1995.
- 39 Jurdao, S., Yebra, M., Guerschman, J. P., and Chuvieco, E.: Regional estimation of woodland  
40 moisture content by inverting Radiative Transfer Models, Remote Sensing of Environment,  
41 132, 59-70, <http://dx.doi.org/10.1016/j.rse.2013.01.004>, 2013.
- 42 Law, B., Arkebauer, T., Campbell, J., Chen, J., Sun, O., Schwartz, M., van Ingen, C., and  
43 Verma, S.: Terrestrial carbon observations: protocols for vegetation sampling and data

- 1 submission, Terrestrial Carbon Observations Panel of the Global Terrestrial Observing  
2 System, Rome, Italy, 2008.
- 3 ~~MacArthur, A., MacLellan, C. J., and Malthus, T.: The Fields of View and Directional~~  
4 ~~Response Functions of Two Field Spectroradiometers, Geoscience and Remote Sensing, IEEE~~  
5 ~~Transactions on, 50, 3892-3907, 10.1109/tgrs.2012.2185055, 2012.~~
- 6 Paltridge, G. W., and Barber, J.: Monitoring grassland dryness and fire potential in australia  
7 with NOAA/AVHRR data, Remote Sensing of Environment, 25, 381-394,  
8 [http://dx.doi.org/10.1016/0034-4257\(88\)90110-1](http://dx.doi.org/10.1016/0034-4257(88)90110-1), 1988.
- 9 Peñuelas, J., Savé, R., Marfà, O., and Serrano, L.: Remotely measured canopy temperature of  
10 greenhouse strawberries as indicator of water status and yield under mild and very mild water  
11 stress conditions, Agricultural and Forest Meteorology, 58, 63 - 77, 1992.
- 12 Peterson, S. H., Roberts, D. A., and Dennison, P. E.: Mapping live fuel moisture with MODIS  
13 data: A multiple regression approach, Remote Sensing of Environment, 112, 4272-4284,  
14 <http://dx.doi.org/10.1016/j.rse.2008.07.012>, 2008.
- 15 Pinty, B., and Verstraete, M. M.: GEMI: a non-linear index to monitor global vegetation from  
16 satellites, Plant Ecology, 101, 15-20, 1992.
- 17 Riaño, D., Vaughan, P., Chuvieco, E., Zarco-Tejada, P. J., and Ustin, S. L.: Estimation of fuel  
18 moisture content by inversion of radiative transfer models to simulate equivalent water  
19 thickness and dry matter content: analysis at leaf and canopy level, Geoscience and Remote  
20 Sensing, IEEE Transactions on, 43, 819-826, 10.1109/tgrs.2005.843316, 2005.
- 21 Richter, K., Atzberger, C., Hank, T. B., and Mauser, W.: Derivation of biophysical variables  
22 from Earth observation data: validation and statistical measures, APPRES, 6, 063557-063551-  
23 063557-063523, 10.1117/1.jrs.6.063557, 2012.
- 24 Roberts, D. A., Dennison, P. E., Peterson, S., Sweeney, S., and Rechel, J.: Evaluation of  
25 Airborne Visible/Infrared Imaging Spectrometer (AVIRIS) and Moderate Resolution Imaging  
26 Spectrometer (MODIS) measures of live fuel moisture and fuel condition in a shrubland  
27 ecosystem in southern California, Journal of Geophysical Research: Biogeosciences, 111,  
28 G04S02, 10.1029/2005jg000113, 2006.
- 29 Rouse, J. W., Haas, R. H., Deering, D. W., and Schell, J. A.: Monitoring the vernal  
30 advancement and retrogradation (green wave effect) of natural vegetation, Goddard Space  
31 Flight Center, Greenbelt, MD, 87, 1973.
- 32 Sepulcre-Cantó, G., Zarco-Tejada, P. J., Jiménez-Muñoz, J. C., Sobrino, J. A., de Miguel, E.,  
33 and Villalobos, F. J.: Detection of water stress in an olive orchard with thermal remote  
34 sensing imagery, Agricultural and Forest Meteorology, 136, 31 - 44, 2006.
- 35 Sims, D. A., and Gamon, J. A.: Estimation of vegetation water content and photosynthetic  
36 tissue area from spectral reflectance: a comparison of indices based on liquid water and  
37 chlorophyll absorption features, Remote Sensing of Environment, 84, 526-537,  
38 [http://dx.doi.org/10.1016/S0034-4257\(02\)00151-7](http://dx.doi.org/10.1016/S0034-4257(02)00151-7), 2003.
- 39 Steyerberg, E. W., Harrell Jr, F. E., Borsboom, G. J. J. M., Eijkemans, M. J. C., Vergouwe,  
40 Y., and Habbema, J. D. F.: Internal validation of predictive models: Efficiency of some  
41 procedures for logistic regression analysis, Journal of Clinical Epidemiology, 54, 774-781,  
42 [http://dx.doi.org/10.1016/S0895-4356\(01\)00341-9](http://dx.doi.org/10.1016/S0895-4356(01)00341-9), 2001.



- 1 Stow, D., Niphadkar, M., and Kaiser, J.: MODIS-derived visible atmospherically resistant  
2 index for monitoring chaparral moisture content, *International Journal of Remote Sensing*, 26,  
3 3867-3873, 10.1080/01431160500185342, 2005.
- 4 Stow, D., Niphadkar, M., and Kaiser, J.: Time series of chaparral live fuel moisture maps  
5 derived from MODIS satellite data, *International Journal of Wildland Fire*, 15, 347-360,  
6 <http://dx.doi.org/10.1071/WF05060>, 2006.
- 7 Taiz, L., and Zeiger, E.: *Plant Physiology*, Sinauer Associates, Incorporated, Sunderland,  
8 2010.
- 9 Trombetti, M., Riaño, D., Rubio, M. A., Cheng, Y. B., and Ustin, S. L.: Multi-temporal  
10 vegetation canopy water content retrieval and interpretation using artificial neural networks  
11 for the continental USA, *Remote Sensing of Environment*, 112, 203 - 215, 2008.
- 12 ~~Tucker, C. J.: Red and photographic infrared linear combinations for monitoring vegetation,~~  
13 ~~*Remote Sensing of Environment*, 8, 127-150, 1979.~~
- 14 Verbesselt, J., Somers, B., Lhermitte, S., Jonckheere, I., van Aardt, J., and Coppin, P.:  
15 Monitoring herbaceous fuel moisture content with SPOT VEGETATION time-series for fire  
16 risk prediction in savanna ecosystems, *Remote Sensing of Environment*, 108, 357 - 368, 2007.
- 17 Wolfe, R. E., Nishihama, M., Fleig, A. J., Kuyper, J. A., Roy, D. P., Storey, J. C., and Patt, F.  
18 S.: Achieving sub-pixel geolocation accuracy in support of MODIS land science, *Remote*  
19 *Sensing of Environment*, 83, 31-49, [http://dx.doi.org/10.1016/S0034-4257\(02\)00085-8](http://dx.doi.org/10.1016/S0034-4257(02)00085-8), 2002.
- 20 Yebra, M., Chuvieco, E., and Aguado, I.: Comparación entre modelos empíricos y de  
21 transferencia radiativa para estimar contenido de humedad en pastizales: Poder de  
22 generalización, *Revista de Teledetección*, 29, 73-90, 2008a.
- 23 Yebra, M., Chuvieco, E., and Riaño, D.: Estimation of live fuel moisture content from  
24 MODIS images for fire risk assessment, *Agricultural and Forest Meteorology*, 148, 523 - 536,  
25 2008b.
- 26 Yebra, M., Dennison, P. E., Chuvieco, E., Riaño, D., Zylstra, P., Hunt Jr, E. R., Danson, F.  
27 M., Qi, Y., and Jurdao, S.: A global review of remote sensing of live fuel moisture content for  
28 fire danger assessment: Moving towards operational products, *Remote Sensing of*  
29 *Environment*, 136, 455-468, <http://dx.doi.org/10.1016/j.rse.2013.05.029>, 2013.
- 30 Zarco-Tejada, P. J., Rueda, C. A., and Ustin, S. L.: Water content estimation in vegetation  
31 with MODIS reflectance data and model inversion methods, *Remote Sensing of Environment*,  
32 85, 109 - 124, 2003.



1 Table 1: Spectral indices calculated using field ~~reflectance~~-HCRF measurements and MODIS  
2 data.  $B_x$  designates the band number corresponding to the MOD09GA product surface  
3 reflectance product.

Index	Formula	Reference
Normalized difference vegetation index (NDVI)	$NDVI = \frac{B_2 - B_1}{B_2 + B_1}$	(Rouse et al., 1973)
Enhanced Vegetation Index (EVI)	$EVI = 2.5 \cdot \left( \frac{B_2 - B_1}{B_2 + 6 \cdot B_1 - 7.5 \cdot B_3} \right)$	(Huete et al., 2002)
Normalized Difference Water Index (NDWI)	$NDWI = \frac{B_2 - B_5}{B_2 + B_5}$	(Gao, 1996)
Normalized Difference Infrared Index (NDII)	$NDII = \frac{B_2 - B_6}{B_2 + B_6}$	(Hardisky et al., 1983)
Simple Ratio Water Index (SRWI)	$SRWI = \frac{B_2}{B_5}$	(Zarco- Tejada et al., 2003)
Soil Adjusted Vegetation Index (SAVI)	$SAVI = \left( \frac{B_2 - B_1}{B_2 + B_1 + L} \right) \cdot (1 + L)$ Where $L = 0.5$	(Huete, 1988)
Global Environment Monitoring Index (GEMI)	$GEMI = \eta \cdot (1 - 0.25\eta) - \frac{B_1 - 0.125}{1 - B_1}$ $\eta = \frac{2 \cdot (B_2^2 - B_1^2) + 1.5 \cdot B_2 + 0.5 \cdot B_2}{B_2 + B_1 + 0.5}$ where	(Pinty and Verstraete, 1992)
Visible Atmospherically Resistant Index (VARI)	$VARI = \frac{B_4 - B_1}{B_4 + B_1 - B_3}$	(Gitelson et al., 2002a)

Global Monitoring (GVMI)	Vegetation Index	$GVMI = \frac{\left(NIR_{REC}^* + 0.1\right) - \left(SWIR - 0.02\right)}{\left(NIR_{REC}^* + 0.1\right) + \left(SWIR - 0.02\right)}$	(Ceccato et al., 2002)
--------------------------------	---------------------	--	------------------------

Central band wavelength	B1= 645.5 nm, B2= 856.5 nm, B3= 465.6 nm, B4= 553.6 nm, B5= 1241.6 nm, B6= 1629.1 nm, B7= 2114.1 nm
----------------------------	---

- 
- |   |  |
|---|--|
| 1 | <ul style="list-style-type: none"> <li>NIR<sub>REC</sub> stands for the information in the Near Infra Red rectified as the index was designed for SPOT-VEGETATION (Ceccato et al., 2002). In this study the index was calculated using the spectral bands from MODIS corresponding to that B2 for the NIR and B5 for the SWIR regions</li> </ul> |
| 2 |  |
| 3 |  |
| 4 |  |

1

Table 2: Empirical fitting equations obtained after bootstrap.

Fitting equation	Fitting equation
Proximal Sensing	MODIS
$FMC_{OQ} = (1184.400 \cdot GEMI) - 734.405$	$FMC_{OQ} = (1727.326 \cdot EVI) - 216.433$
$FMC_{IQ} = (999.707 \cdot GEMI) - 626.932$	$FMC_{IQ} = (1398.385 \cdot EVI) - 173.518$
$EWT = (0.029 \cdot EVI) + 0.011$	$EWT = (0.059 \cdot EVI) + 0.003$
$LAI = (2.621 \cdot NDII) + 1.268$	$LAI = (3.524 \cdot NDII) + 1.189$
$CWC_{OQ} = (0.075 \cdot NDII) + 0.029$	$CWC_{OQ} = (0.195 \cdot EVI) - 0.032$
$CWC_{IQ} = (0.063 \cdot NDII) + 0.023$	$CWC_{IQ} = (0.157 \cdot EVI) - 0.026$

2

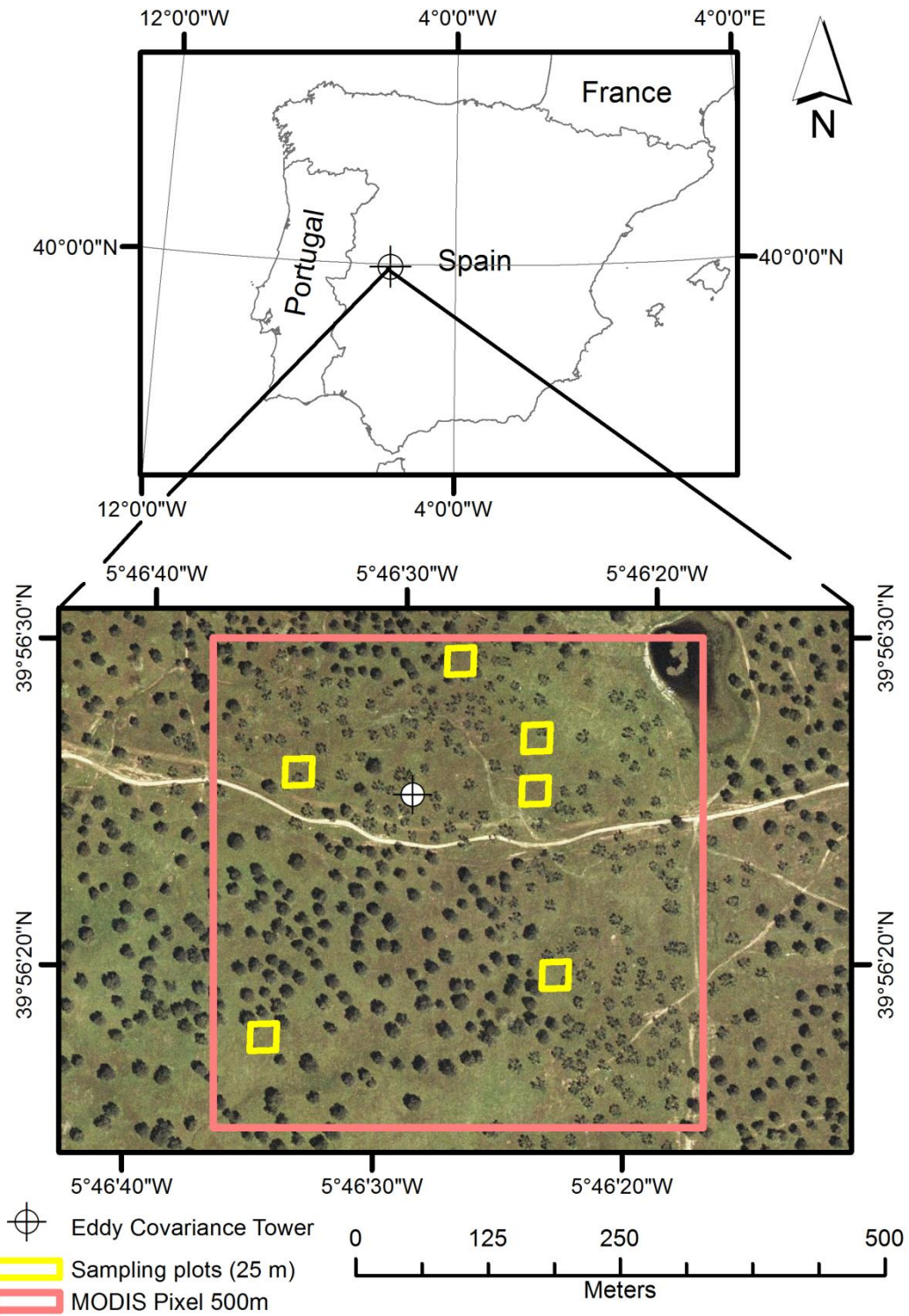
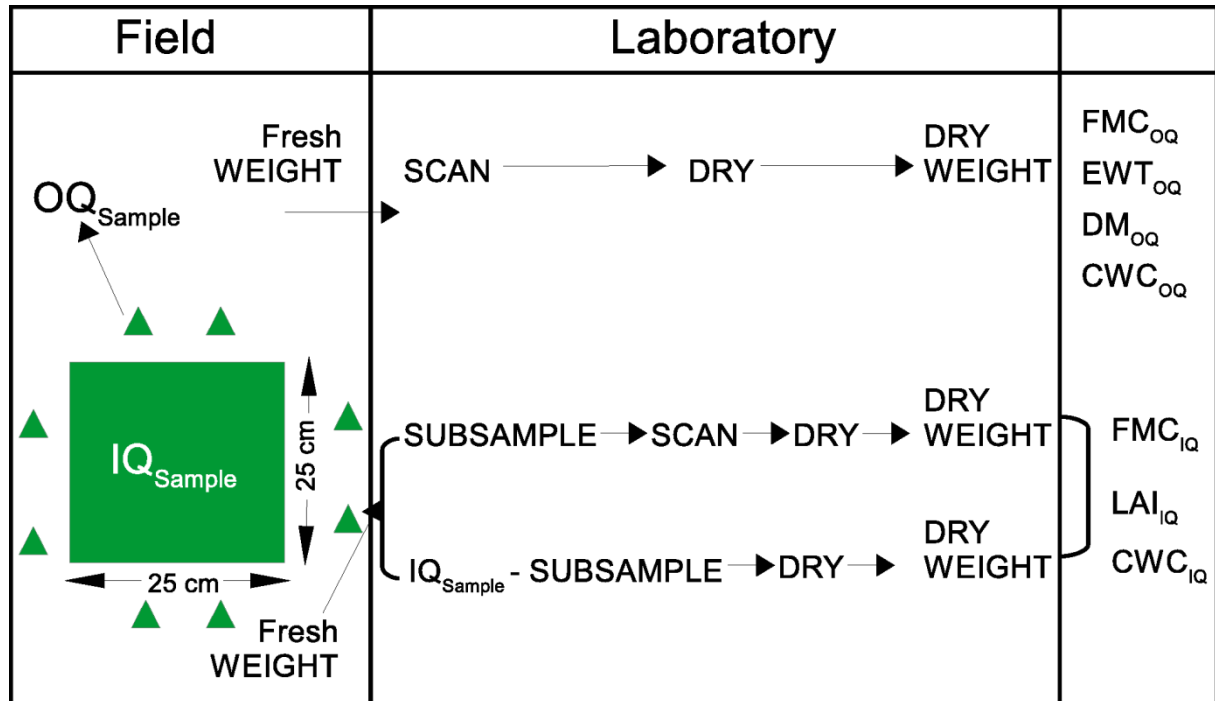


Figure 1. Plots sampled near the FLUXNET tower within the 500 m MODIS pixel at Las Majadas del Tiétar (Spain) study site.

1



2

3

4 Figure 2. Scheme showing the different samples collected in the field and how they are  
 5 processed in the laboratory. Metrics obtained as results are also indicated in the last column.

6

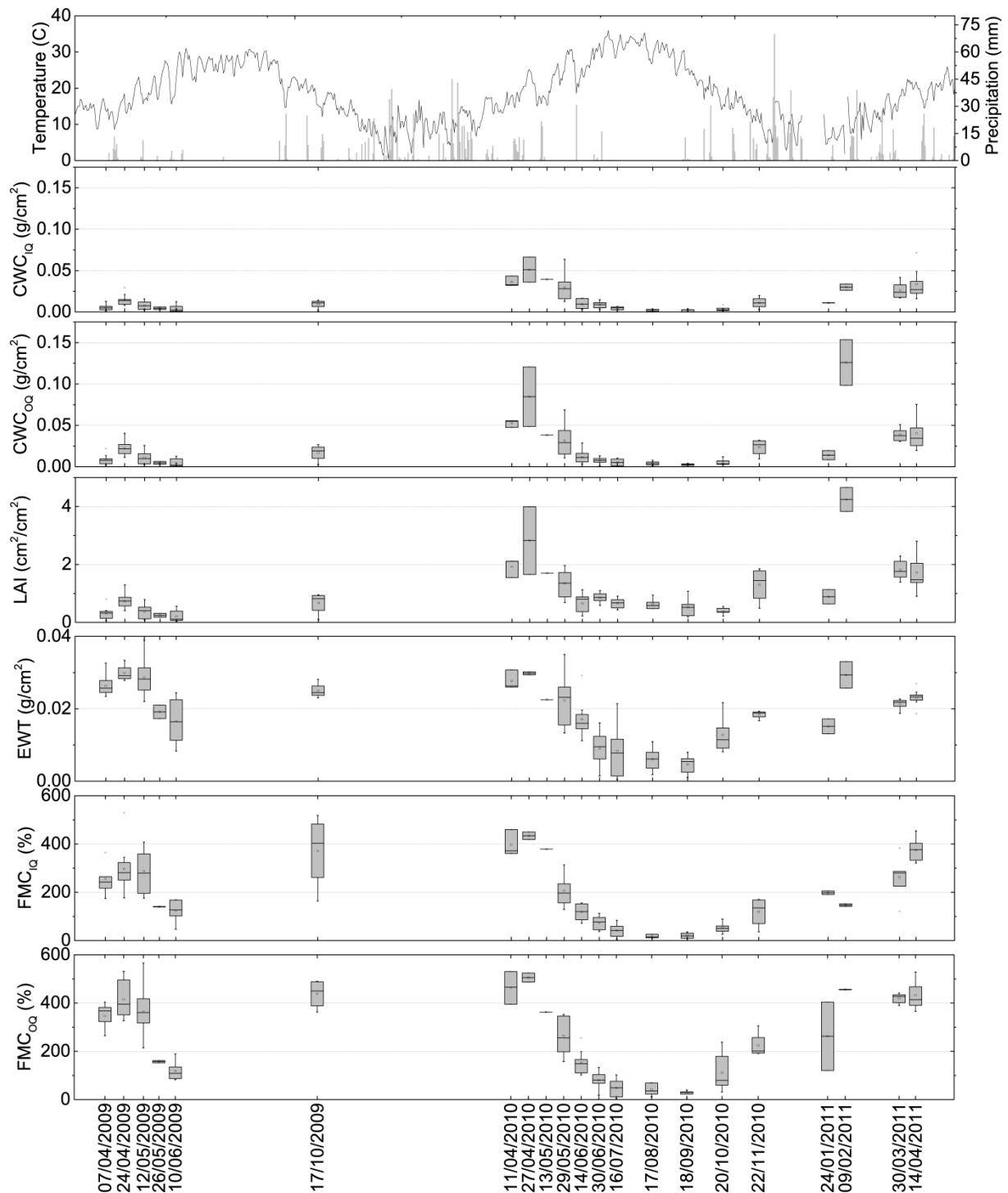


Figure 3. Box plot showing the temporal evolution of field biophysical variables measured. Filled points represent the median of the daily measurements, the boxes indicate the position of the 1st and 3rd quartile, lines delimit the maximum and minimum values, and empty points are outliers. Line inside the boxes showed the median value of the day and the point the mean value. Precipitation is represented using bars and temperature is represented with a solid line

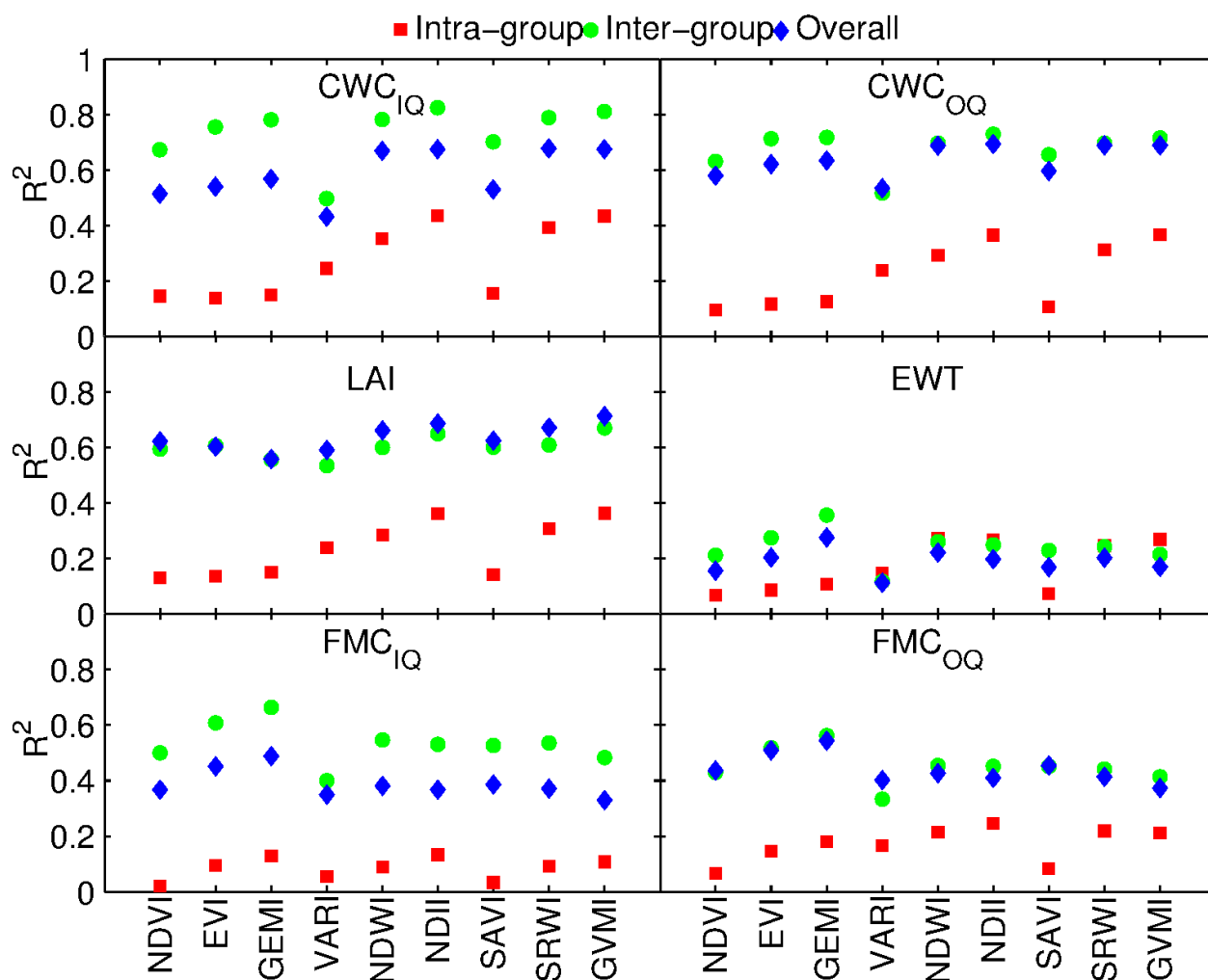


Figure 4. Intra-group, inter-group and overall  $R^2$  values between proximal sensing spectral indexes and biophysical variables measured in the field.



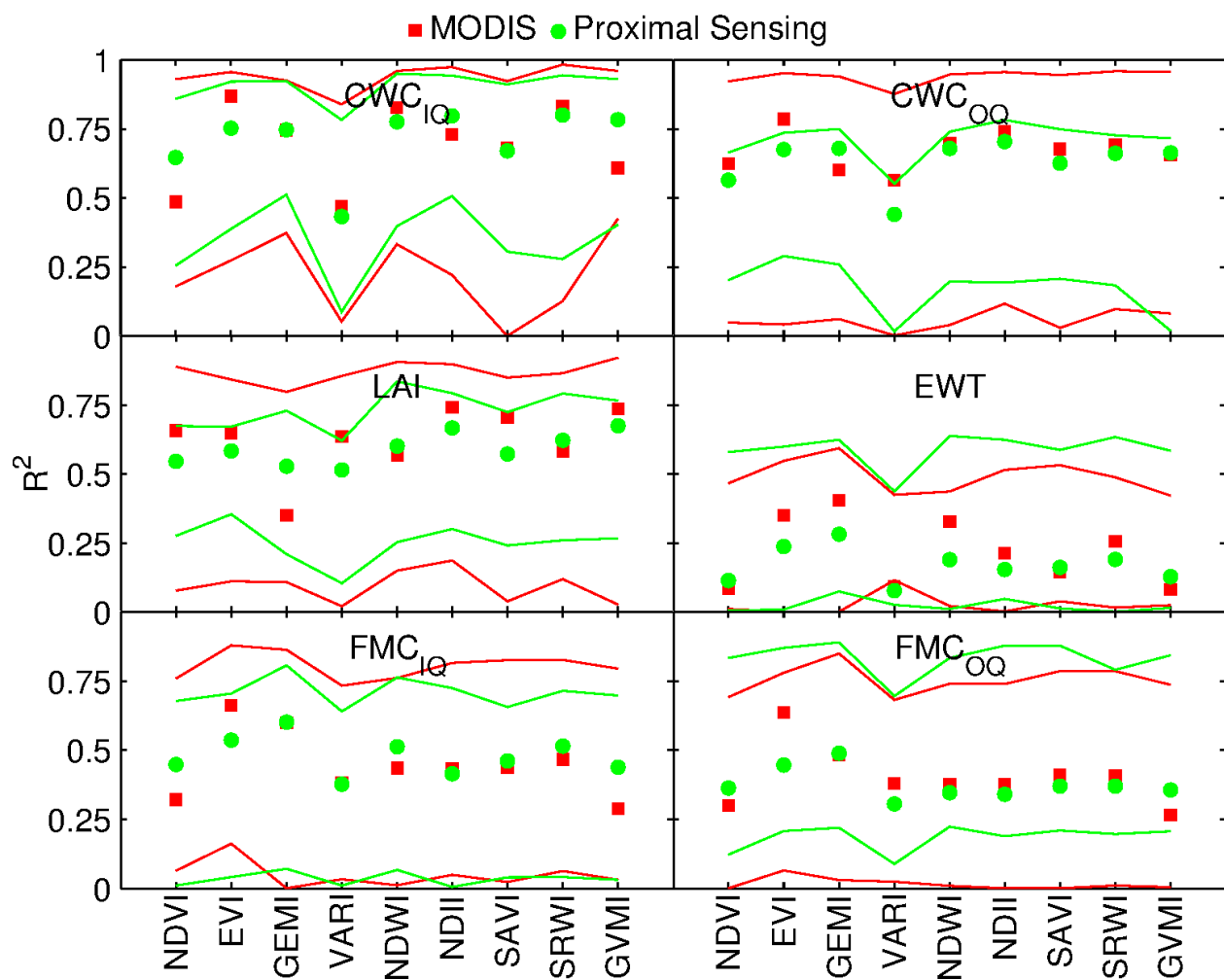


Figure 5. Model performance statistics for all the spectral indices calculated using proximal sensing-termination coefficient for proximal (green circles) and MODIS (red squares) empirical models after bootstrap. Upper and lower limits of the confidence intervals for MODIS and proximal sensing are presented.

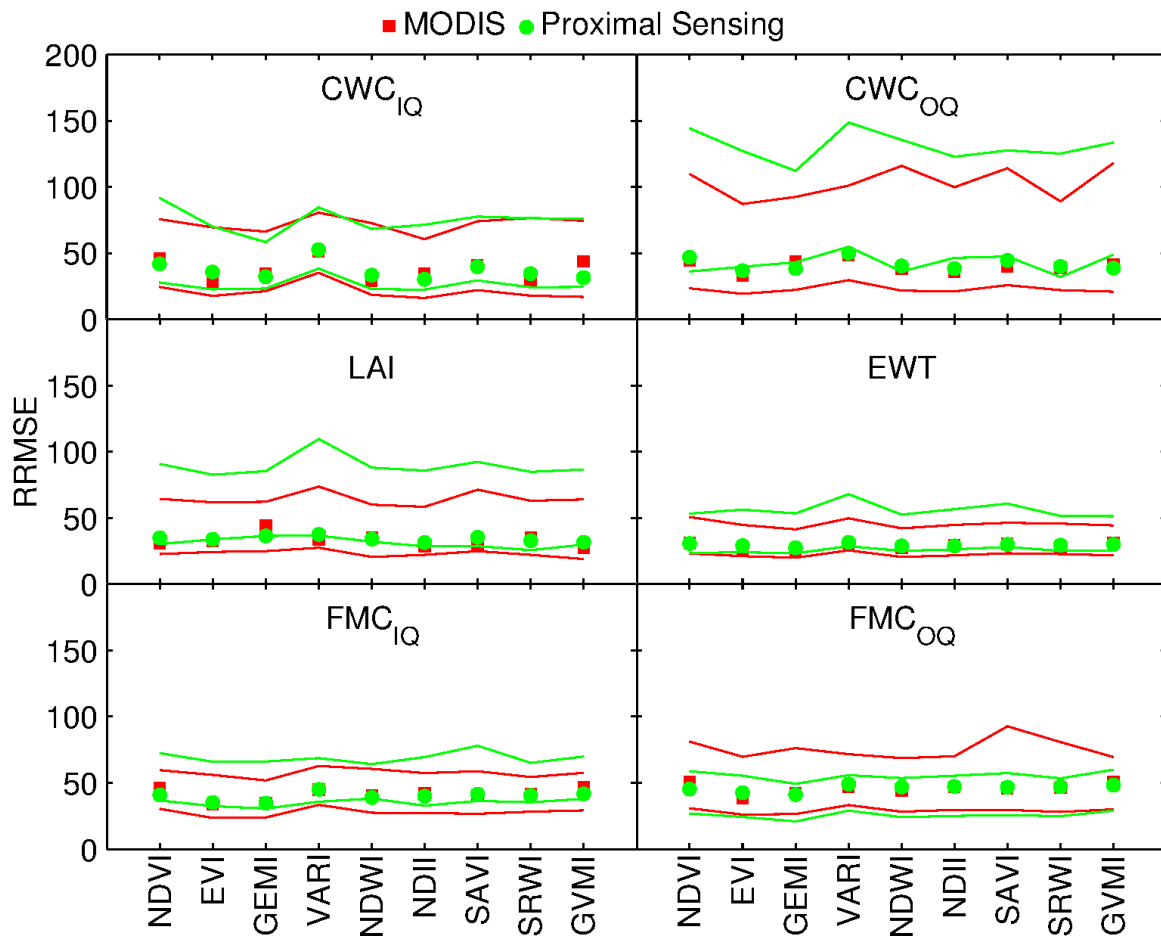


Figure 6. Relative root mean square error for proximal (green circles) and MODIS (red squares) empirical models after bootstrap. Upper and lower limits of the confidence intervals for MODIS and Proximal sensing are presented. ~~Model performance statistics for all the spectral indices calculated using MODIS data.~~

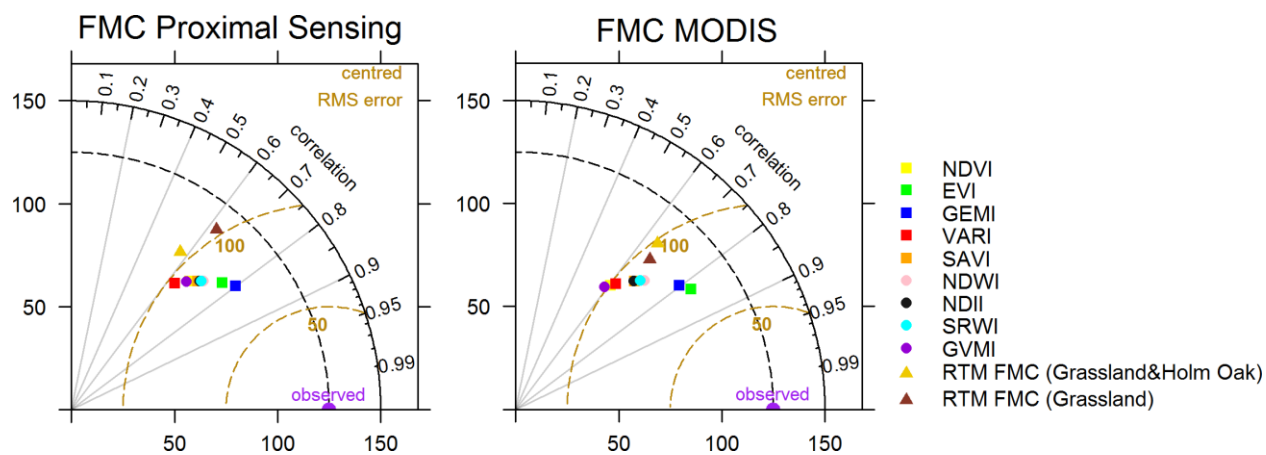


Figure 7. Comparison of empirical vs RTM models to estimate FMC with proximal sensing (left) and MODIS (right). RTM FMC (Grassland) obtained from the LUT proposed by (Yebara et al., 2008b). RTM FMC (Grassland& Holm Oak) obtained from the LUT proposed by Jurdao et al. (2013).

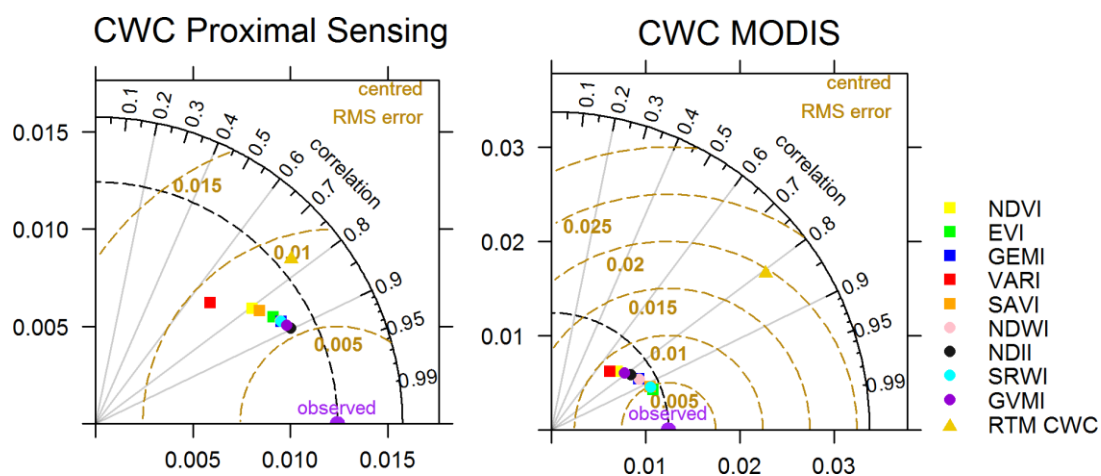


Figure 8. Comparison of empirical vs RTM models to estimate CWC with proximal sensing (left) and MODIS (right). RTM CWC is based on Trombetti et al. (2008).

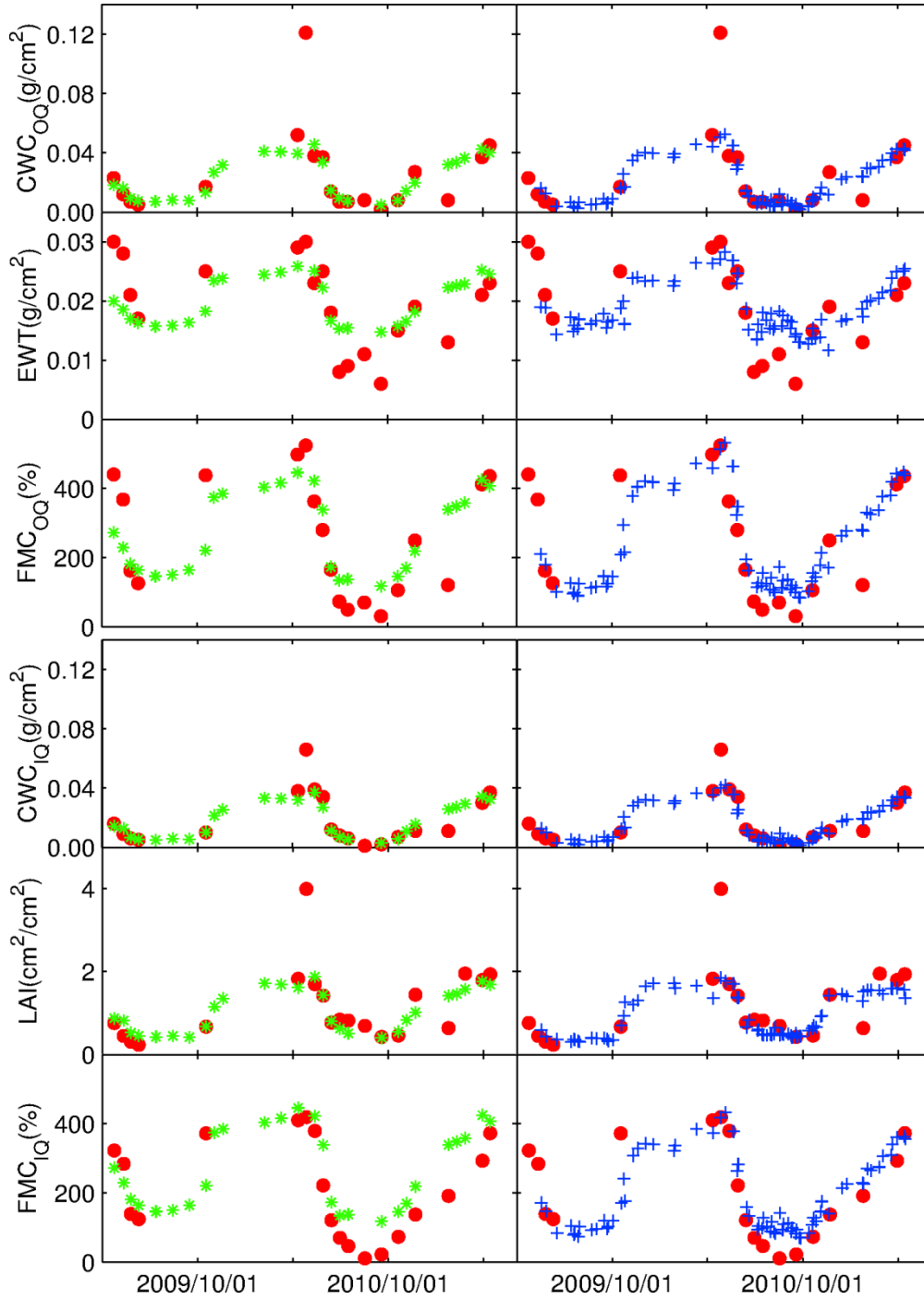


Figure 9. Temporal evolution of the observed (red circles) and estimated FMC<sub>OQ</sub>, FMC<sub>IQ</sub>, EWT, LAI, CWC<sub>OQ</sub> and CWC<sub>IQ</sub> obtained for proximal sensing (green asterisks) and MODIS (blue crosses). Fitting equations are presented in Table 2.